Recent Results from the CSSM

Anthony G. Williams

3rd Topical Workshop on Lattice Hadron Physics (LHP06), Jefferson Lab, Newport News, Virginia, USA, July 31 – August 3, 2006

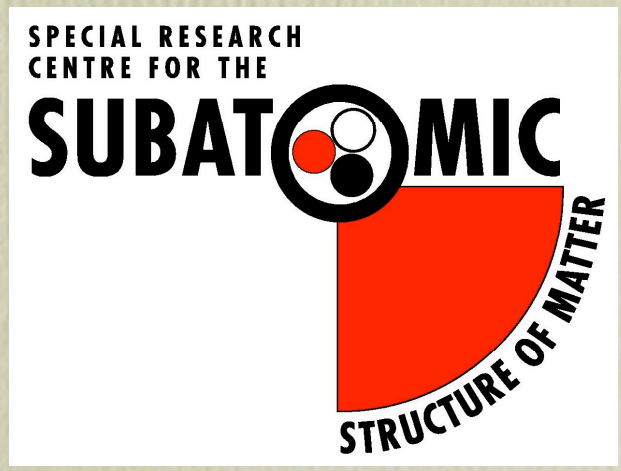

Contents

- Introduction - status and future of the CSSM
- Brief summary of current CSSM research
- Lattice QCD: CSSM Lattice Collaboration
  - Baryon spectrum: ground and excited states (Ben L)
  - Search for spin 1/2 and 3/2 pentaquarks (Ben L)
  - QCD vacuum structure and flux tubes (Derek L)
  - E.m. form factors of octet and decuplet baryons
  - Dynamical FLIC and other fermions
  - Form factors of mesons
  - Search for the 1^{-+} and other Exotic Meson
  - Quark and gluon Green's functions
- Conclusions

Status & Future of the CSSM

- The CSSM is the ARC Special Research Centre for the Subatomic Structure of Matter
- Funded as an SRC for 1997-2005 - the ARC explicitly provides for the use CSSM title in 2006 and beyond
- Founders: Tony Thomas (Director, now at JLab as Theory Head & Scientific Director) & Tony Williams (Deputy Director, now Director)
- Current key academic staff: Tony Williams (Dir); Derek Leinweber (Dep Dir); Lorenz von Smekal.
- Other affiliate academic staff: Rod Crewther; Ray Protheroe; Max Lohe.
- Current postdoctoral fellows: Ayse Kizilersu, Alan O'Cais; Andre Sternbeck; Ben Lasscock (soon, for 1 year).

Status & Future of the CSSM

- Current graduate students: Sharada Boinepalli (submitted); Jonathan Carroll; James Chappell; Ian Cloet; Ben Crouch; Marco Ghiotti; John Hedditch (submitted); Mariusz Hoppe; Dhagash Metha; Ben Lasscock (submit soon); Sarah Lawley; Selim Mahbub; Bao-Loc Nguyen; Maria Parappilly (submitted); Skye Platten.
- From 2006 the CSSM will be funded by ARC Discovery Project, LIEF, Linkage grants etc.
- Current funding from ARC grants approx 60% of CSSM funding - core physics programs maintained
- Most but not all of the CSSM research program focuses on studies of QCD and the strong interactions
- In particular, the CSSM hosts a key lattice QCD group – the CSSM Lattice Collaboration
- Uses the computing resources of SAPAC and APAC

Status & Future of the CSSM

- CSSM Lattice Collaboration has access to computing resources from SAPAC and APAC
- APAC (typically CSSM uses 10% of cycles): at ANU in Canberra, currently an SGI Altix, (1680 Itanium2 1.6GHz on NUMA), 10 Teraflops peak; next upgrade approx to 100 Teraflops in 2 years.
- SAPAC (typically CSSM uses 50% of total cycles):
  i. IBM1350 (129 dual Xeon nodes on Myrinet), 1.2 Teraflop peak;
  ii. SGI Altix (160 Itanium2 1.3GHz on NUMA), 0.83 Teraflops peak;
  iii. New cluster to be purchase Q4 2006, anticipate dual core on infiniband, approx 4 Teraflops peak.

Summary : The CSSM alive and well post "block funding" and has a healthy long-term future ahead.

Brief summary of current CSSM research

- CSSM Lattice Collaboration work - *described later* ;
- Strongly interacting matter at high density - neutron stars, quark and strange stars;
- Odd-parity baryons;
- Dyson-Schwinger equations and infrared behavior of QCD Green's functions - confinement, triviality of QED4, etc.;
- Fundamental formulation of gauge field theories - BRST, Gribov copies, Neuberger problem, gauge-fixing;
- Chiral extrapolations and effective field theory;

Plus some efforts not in the particle-nuclear field:

- Spin glasses, scale free networks, econophysics etc.;
- Protein folding - Nose-Hoover algorithm, multi-body problem in contact with heat bath;
- Quantum computing.

Lattice QCD: CSSM Lattice Collaboration Studies

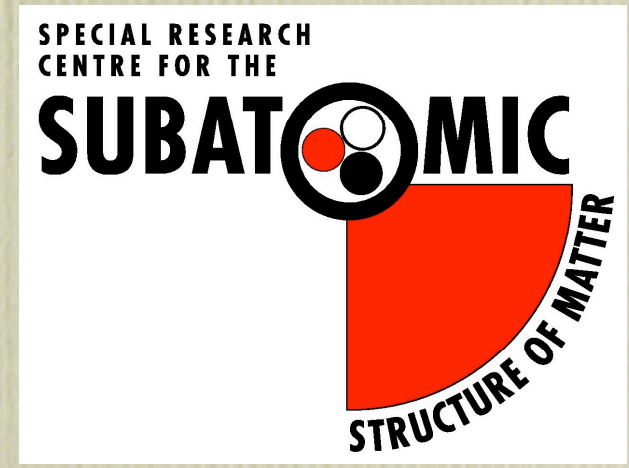

Lattice QCD: CSSM Lattice Collaboration Studies

- Baryon spectrum: ground and excited states (Ben L)
- Search for spin 1/2 and 3/2 pentaquarks (Ben L)
- QCD vacuum structure and flux tubes (Derek L)
- Electromagnetic structure of octet baryons (here)
- Dynamical FLIC and other fermions (not covered)
- Form factors of mesons (Ben L at Lattice 06 in Tucson)
- Search for the 1^{-+} and other Exotic Meson (brief)
- Quark and gluon Green's functions (brief)

Electromagnetic Structure of Octet Baryons

S. Boinepalli, D.B. Leinweber, A.G. Williams, J.M. Zanotti and J.B. Zhang

CSSM Lattice Collaboration has a primary goal to reveal the electromagnetic structure of baryons near the chiral regime and search for evidence of chiral nonanalytic curvature in accord with quenched chiral effective field theory. Here is some initial work in that direction.

Details of Lattice Simulations

The proton interpolating field is given by

$$\chi^{p+}(x) \;=\; \epsilon^{abc}\left(u^{aT}(x)\; C\gamma_5\; d^b(x)\right) u^c(x)$$

and, e.g., for the Sigma hyperon one uses

$$\chi^{\Sigma^0}(x) = \frac{1}{\sqrt{2}}\epsilon^{abc}\Big\{\left(u^{aT}(x)\; C\gamma_5\; s^b(x)\right) d^c(x) + \left(d^{aT}(x)\; C\gamma_5\; s^b(x)\right) u^c(x)\Big\}$$

The above transforms as an SU(2) isospin triplet .

Replacing “+” with “-” gives an SU(2) isosinglet suitable for the Lambda. An SU(3) octet interpolating field for the Lambda is given by

$$\chi^{\Lambda}(x) = \frac{1}{\sqrt{6}}\epsilon^{abc}\Big\{2\left(u^{aT}(x)\; C\gamma_5\; d^b(x)\right) s^c(x) + \left(u^{aT}(x)\; C\gamma_5\; s^b(x)\right) d^c(x) \;-\; \left(d^{aT}(x)\; C\gamma_5\; s^b(x)\right) u^c(x)\Big\}$$

Correlation functions

The 2-point function is given by

$$\left\langle\, G^{BB}(t;\vec{p},\Gamma)\,\right\rangle = \sum_{\vec{x}} e^{-i\vec{p}\cdot\vec{x}}\,\Gamma^{\beta\alpha}\,\left\langle\,\Omega\,\middle|\,T\left(\chi^{\alpha}(x)\,\overline{\chi}^{\beta}(0)\right)\,\middle|\,\Omega\,\right\rangle$$

and Gamma is a 4x4 spinor matrix. At the hadronic level

$$\left\langle\,\Omega\,\middle|\,\chi(0)\,\middle|\,B,p,s\,\right\rangle = Z_B(p)\sqrt{\frac{M}{E_p}}\,u(p,s)$$

For large Euclidean time we have

$$\left\langle\, G^{BB}(t;\vec{p},\Gamma)\,\right\rangle \simeq \frac{Z_B(p)\overline{Z}_B(p)}{2E_p} e^{-E_p t}\, tr\left[\Gamma(-i\gamma\cdot p + M)\right]$$

Analogously the 3-point function for the e.m. current is

$$\left\langle\, G^{Bj^{\mu}B}(t_2,t_1;\vec{p'},\vec{p};\Gamma)\,\right\rangle =$$

$$\sum_{\vec{x_2},\vec{x_1}} e^{-i\vec{p'}\cdot\vec{x_2}} e^{+i\left(\vec{p'}-\vec{p}\right)\cdot\vec{x_1}}\,\Gamma^{\beta\alpha}\,\left\langle\,\Omega\,\middle|\,T\left(\chi^{\alpha}(x_2)\,j^{\mu}(x_1)\,\overline{\chi}^{\beta}(0)\right)\,\middle|\,\Omega\,\right\rangle\ .$$

Correlation functions (cont.)

For large Euclidean times, $t_2 - t_1 >> 1$ and $t_1 >> 1$, the ground state dominates and one has

$$\langle\, G^{Bj^\mu B}(t_2,t_1;\vec{p'},\vec{p};\Gamma)\,\rangle = \sum_{s,s'} e^{-E_{p'}(t_2-t_1)} e^{-E_p t_1} \Gamma^{\beta\alpha}$$

$$\text{x}\,\langle\,\Omega\,|\,\chi^\alpha\,|\,p',s'\,\rangle\langle\,p',s'\,|\,j^\mu\,|\,p,s\,\rangle\langle\,p,s\,|\,\overline{\chi}^\beta\,|\,\Omega\,\rangle\ .$$

The matrix element of the e.m. current has the form

$$\langle\,p',s'\,|\,j^\mu\,|\,p,s\,\rangle = \left(\frac{M^2}{E_p E_{p'}}\right)^{1/2} \overline{u}(p',s')\left(F_1(q^2)\gamma^\mu - F_2(q^2)\sigma^{\mu\nu}\frac{q^\nu}{2M}\right)u(p,s)$$

To eliminate time-dependence we construct the ratio

$$R(t_2,t_1;\vec{p'},\vec{p};\Gamma,\Gamma';\mu) = \left[\frac{\langle\, G^{Bj^\mu B}(t_2,t_1;\vec{p'},\vec{p};\Gamma)\,\rangle\langle\, G^{Bj^\mu B}(t_2,t_1;-\vec{p},-\vec{p'};\Gamma)\,\rangle}{\langle\, G^{BB}(t_2;\vec{p'};\Gamma')\,\rangle\langle\, G^{BB}(t_2;-\vec{p};\Gamma')\,\rangle}\right]^{1/2}$$

and further define

$$\overline{R}(\vec{p'},\vec{p};\Gamma,\Gamma';\mu) = \left[\frac{2E_p}{E_p+M}\right]^{1/2}\left[\frac{2E_{p'}}{E_{p'}+M}\right]^{1/2} R(t_2,t_1;\vec{p'},\vec{p};\Gamma,\Gamma';\mu)$$

Correlation functions (cont.)

Noting that the e.m current

$$\langle\, p', s' \mid j^{\mu} \mid p, s \,\rangle = \left(\frac{M^2}{E_p E_{p'}}\right)^{1/2} \overline{u}(p', s') \left(F_1(q^2)\gamma^{\mu} - F_2(q^2)\sigma^{\mu\nu}\frac{q^{\nu}}{2M}\right) u(p, s)$$

It is readily shown that

$$\begin{aligned}
\mathcal{G}_E(q^2) &= \overline{R}(\vec{q}, \vec{0}; \Gamma_4, \Gamma_4, 4)\,, \\
|\epsilon_{ijk} q^i|\, \mathcal{G}_M(q^2) &= (E_q + M)\, \overline{R}(\vec{q}, \vec{0}; \Gamma_j, \Gamma_4, k)\,, \\
|q^k|\, \mathcal{G}_E(q^2) &= (E_q + M)\, \overline{R}(\vec{q}, \vec{0}; \Gamma_4, \Gamma_4, k)\,,
\end{aligned}$$

where $\Gamma_j = \frac{1}{2}\begin{pmatrix} \sigma_j & 0 \\ 0 & 0 \end{pmatrix}$ $\Gamma_4 = \frac{1}{2}\begin{pmatrix} I & 0 \\ 0 & 0 \end{pmatrix}$

and from which the Sachs form factors can be obtained

$$\begin{aligned}
\mathcal{G}_E(q^2) &= F_1(q^2) - \frac{q^2}{(2M)^2} F_2(q^2)\,, \\
\mathcal{G}_M(q^2) &= F_1(q^2) + F_2(q^2)\,,
\end{aligned}$$

Correlation fns at quark level

Want to study quark-level contributions to probe hadron substructure and inform quark models.

Requires decomposing correlation functions into quark components.

Define a function of three quark propagators, S_f, for convenience as

$$\mathcal{G}(S_{f_1}, S_{f_2}, S_{f_3}) \equiv \epsilon^{abc}\epsilon^{a'b'c'}\left\{S_{f_1}^{aa'}(x,0)\,\mathrm{tr}\left[S_{f_2}^{bb'\,T}(x,0)S_{f_3}^{cc'}(x,0)\right] + S_{f_1}^{aa'}(x,0)\,S_{f_2}^{bb'\,T}(x,0)\,S_{f_3}^{cc'}(x,0)\right\}$$

Using this we can the write, e.g., the proton channel 2-point correlation function in a shorthand form

$$G^{p+}(t,\vec{p};\Gamma) = \left\langle \sum_{\vec{x}} e^{-i\vec{p}\cdot\vec{x}}\mathrm{tr}\left[\Gamma\ \mathcal{G}\left(S_u,\ \widetilde{C}S_d\widetilde{C}^{-1},\ S_u\right)\right]\right\rangle$$

and more complicated but similar forms for other baryon channels.

Correlation fns at quark level

For example, the correlation function for the SU(3) octet Lambda interpolating field can be written as

$$G^{\Lambda^8}(t,\vec{p};\Gamma) = \frac{1}{6}\sum_{\vec{x}} e^{-i\vec{p}\cdot\vec{x}}\mathrm{tr}\Big[\Gamma\Big\{\,2\,\mathcal{G}\left(S_s,\,\widetilde{C}S_u\widetilde{C}^{-1},\,S_d\right)+2\,\mathcal{G}\left(S_s,\,\widetilde{C}S_d\widetilde{C}^{-1},\,S_u\right)$$
$$+\,2\,\mathcal{G}\left(S_d,\,\widetilde{C}S_u\widetilde{C}^{-1},\,S_s\right)+2\,\mathcal{G}\left(S_u,\,\widetilde{C}S_d\widetilde{C}^{-1},\,S_s\right)$$
$$-\;\;\mathcal{G}\left(S_d,\,\widetilde{C}S_s\widetilde{C}^{-1},\,S_u\right)-\;\;\mathcal{G}\left(S_u,\,\widetilde{C}S_s\widetilde{C}^{-1},\,S_d\right)\Big\}\Big]$$

Correlation fns at quark level

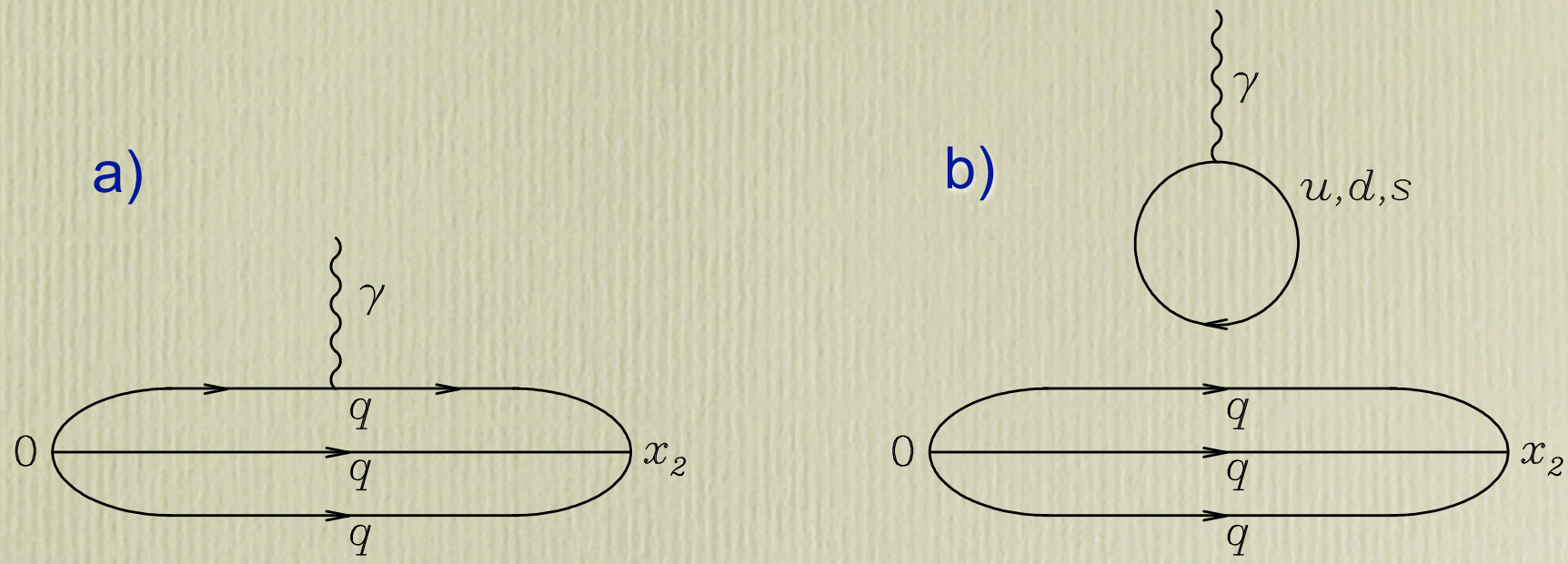

Connected (a) and disconnected (b) contributions to the e.m. form factors in terms of quark flow lines.

In the SU(3) flavor limit the disconnected contributions vanish, since charges sum to zero. We work in the quenched limit here and so only consider connected contributions (a) in any case.

Correlation fns at quark level

Using our shorthand, the 3-point function for, e.g., the proton becomes

$$T\left(\chi^{p+}(x_2)\, j^{\mu}(x_1)\, \overline{\chi}^{p+}(0)\right) =$$

$$\mathcal{G}\left(\widehat{S}_u(x_2,x_1,0),\, \widetilde{C}S_d(x_2,0)\widetilde{C}^{-1},\, S_u(x_2,0)\right) + \mathcal{G}\left(S_u(x_2,0),\, \widetilde{C}S_d(x_2,0)\widetilde{C}^{-1},\, \widehat{S}_u(x_2,x_1,0)\right)$$

$$+\mathcal{G}\left(S_u(x_2,0),\, \widetilde{C}\widehat{S}_d(x_2,x_1,0)\widetilde{C}^{-1},\, S_u(x_2,0)\right)$$

$$+ \sum_{q=u,\,d,\,s} e_q \sum_i tr\left[S_q^{ii}(x_1,x_1)\,\gamma_\mu\right] \mathcal{G}\left(S_u(x_2,0),\, \widetilde{C}S_d(x_2,0)\widetilde{C}^{-1},\, S_u(x_2,0)\right)$$

The 4th piece is the disconnected piece and not calculated. The “caret” (^) on a propagator signifies that it has the e.m. current insertion, i.e., it represents

$$\widehat{S}_q^{aa'}(x_2,x_1,0) = e_q \sum_i S_q^{ai}(x_2,x_1)\,\gamma_\mu\, S_q^{ia'}(x_1,0)\,,$$

In this way we can deconstruct the form factors for each valence quark species in the baryon.

Lattice simulation parameters

- Simulations are performed using the mean-field $O(a^2)$-improved Luscher-Weisz [23] plaquette plus rect-angle gauge action
- $20^3 \times 40$ lattice with periodic boundary conditions.
- Lattice spacing a = 0.128 fm determined by the Sommer scale r0 = 0.50 fm [24].
- Large volume lattice ensures a good density of low- lying momenta which are key to giving rise to chiral non-analytic behaviour in the observables simulated on the lattice.
- 400 configurations

FLIC fermion action

The Fat-Link Irrelevant Clover (FLIC) fermion action is given by

$$S_{\rm SW}^{\rm FL} = S_{\rm W}^{\rm FL} - \frac{i\,g\,C_{\rm SW}\,\kappa\,r}{2(u_0^{\rm FL})^4}\,\bar{\psi}(x)\,\sigma_{\mu\nu}F_{\mu\nu}\,\psi(x)$$

where $F_{\mu\nu}$ is *O(a⁴)* improved using fat links and where the mean-field improved Fat-link Irrelevant Wilson action is given by

$$\begin{aligned} S_{\rm W}^{\rm FL} = \sum_x\ \bar{\psi}(x)\psi(x) + \kappa\sum_{x,\mu}\bar{\psi}(x)\Bigg[\gamma_\mu\left(\frac{U_\mu(x)}{u_0}\psi(x+\hat{\mu})\right. \\ \left. - \frac{U_\mu^\dagger(x-\hat{\mu})}{u_0}\psi(x-\hat{\mu})\right) - r\left(\frac{U_\mu^{\rm FL}(x)}{u_0^{\rm FL}}\psi(x+\hat{\mu})\right. \\ \left. + \frac{U_\mu^{\rm FL\dagger}(x-\hat{\mu})}{u_0^{\rm FL}}\psi(x-\hat{\mu})\right)\Bigg] \end{aligned}$$

Kappa values and masses

TABLE I: Hadron masses in appropriate powers of GeV for various values of the hopping parameter, κ. For reference, experimentally measured values are indicated at the end of the table.

κ	m_π^2	N	Λ	Σ	Ξ
0.12630	0.9972(55)	1.829(8)	1.728(10)	1.700(9)	1.612(11)
0.12680	0.8947(54)	1.763(9)	1.681(10)	1.656(10)	1.586(12)
0.12730	0.7931(53)	1.695(9)	1.632(11)	1.566(11)	1.558(12)
0.12780	0.6910(35)	1.629(10)	1.584(10)	1.570(10)	1.531(10)
0.12830	0.5925(33)	1.554(10)	1.530(10)	1.521(10)	1.502(10)
0.12885	0.4854(31)	1.468(11)	1.468(11)	1.468(11)	1.468(11)
0.12940	0.3795(31)	1.383(11)	1.406(11)	1.417(11)	1.435(11)
0.12990	0.2839(33)	1.301(11)	1.347(11)	1.371(11)	1.404(11)
0.13025	0.2153(35)	1.243(12)	1.303(12)	1.341(12)	1.382(11)
0.13060	0.1384(43)	1.190(15)	1.256(13)	1.313(12)	1.359(11)
0.13080	0.0939(44)	1.159(21)	1.226(16)	1.296(14)	1.346(11)
experiment	0.0196	0.939	1.116	1.189	1.315

FLIC conserved vector current

The conserved vector current for the FLIC action constructed using standard Martinelli et al. appproach

$$j_\mu^{\rm CI} \equiv j_\mu^{\rm C}(x) + \frac{r}{2} C_{CVC}\, a \sum_\rho \partial_\rho \big(\overline{\psi}(x)\sigma_{\rho\mu}\psi(x)\big)\,,$$

where the Wilson-type fermion conserved current is

$$\begin{aligned} j_\mu^{\rm C} \;\equiv\; & \frac{1}{4}\big[\overline{\psi}(x)(\gamma_\mu - r)U_\mu(x)\psi(x+\hat{\mu}) \\ & + \;\overline{\psi}(x+\hat{\mu})(\gamma_\mu + r)U_\mu^\dagger(x)\psi(x) \\ & + \;(x \to x-\hat{\mu})\big]. \end{aligned}$$

Proton charge radius

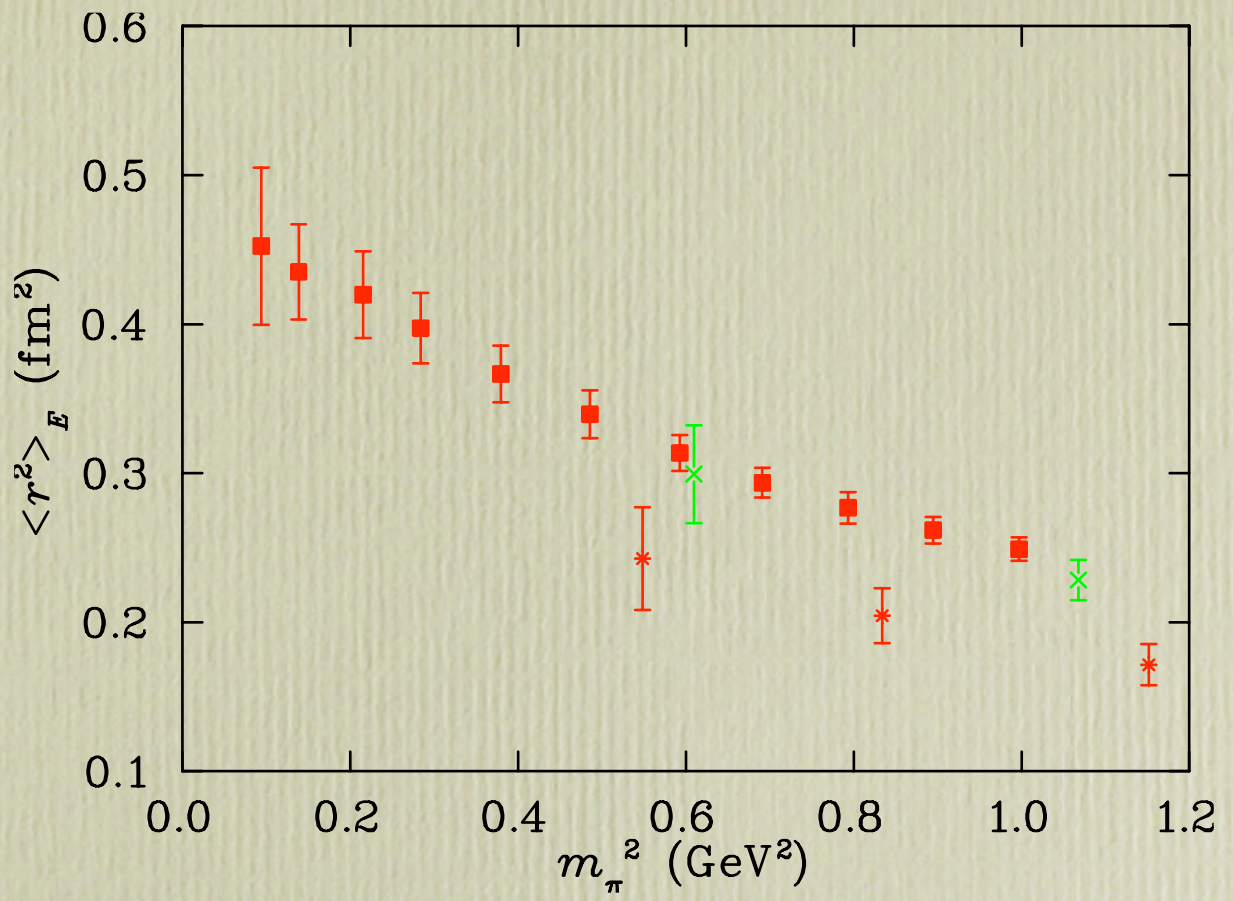

Figure: Proton charge radius compared with previous quenched lattice results. The solid squares indicate current lattice QCD results with FLIC fermions. The stars indicate the lattice results of [Leinweber et al., 1991] while the crosses indicate the results of [Wilcox et al., 1992], both of which use the standard Wilson actions for the gauge and fermion fields.

Proton magnetic moment

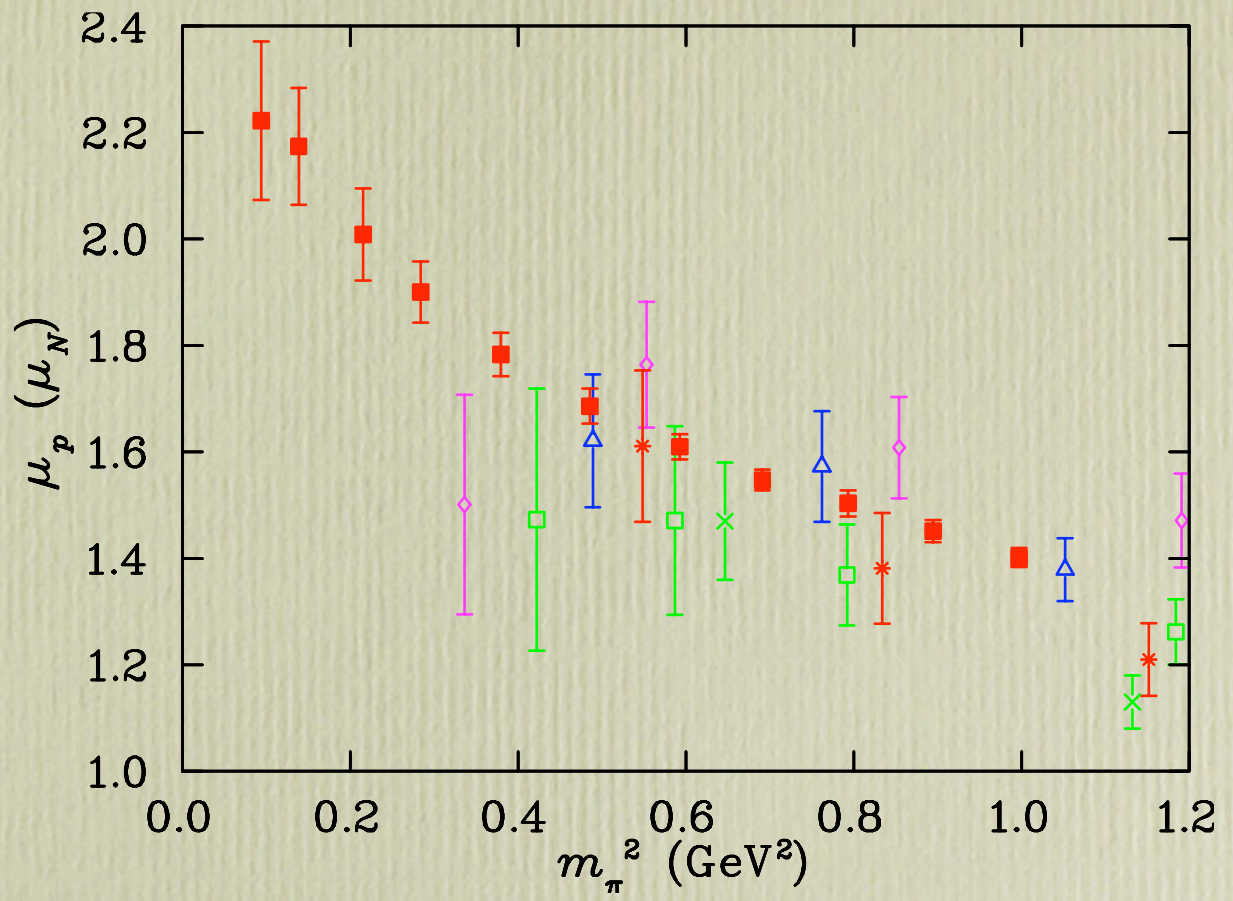

Figure: Proton magnetic moment (in nuclear magnetons) from a variety of lattice simulations. Solid squares = [current FLIC results], stars = [Leinweber et al., 1991], crosses (only one point) = [Wilcox et al., 1992]. Open symbols = [QCDSF collaboration, Gockeler et al., 2005]. Open squares = $\beta = 6.0$, open triangles = $\beta = 6.2$, open diamonds = $\beta = 6.4$.

Strange quark charge radii

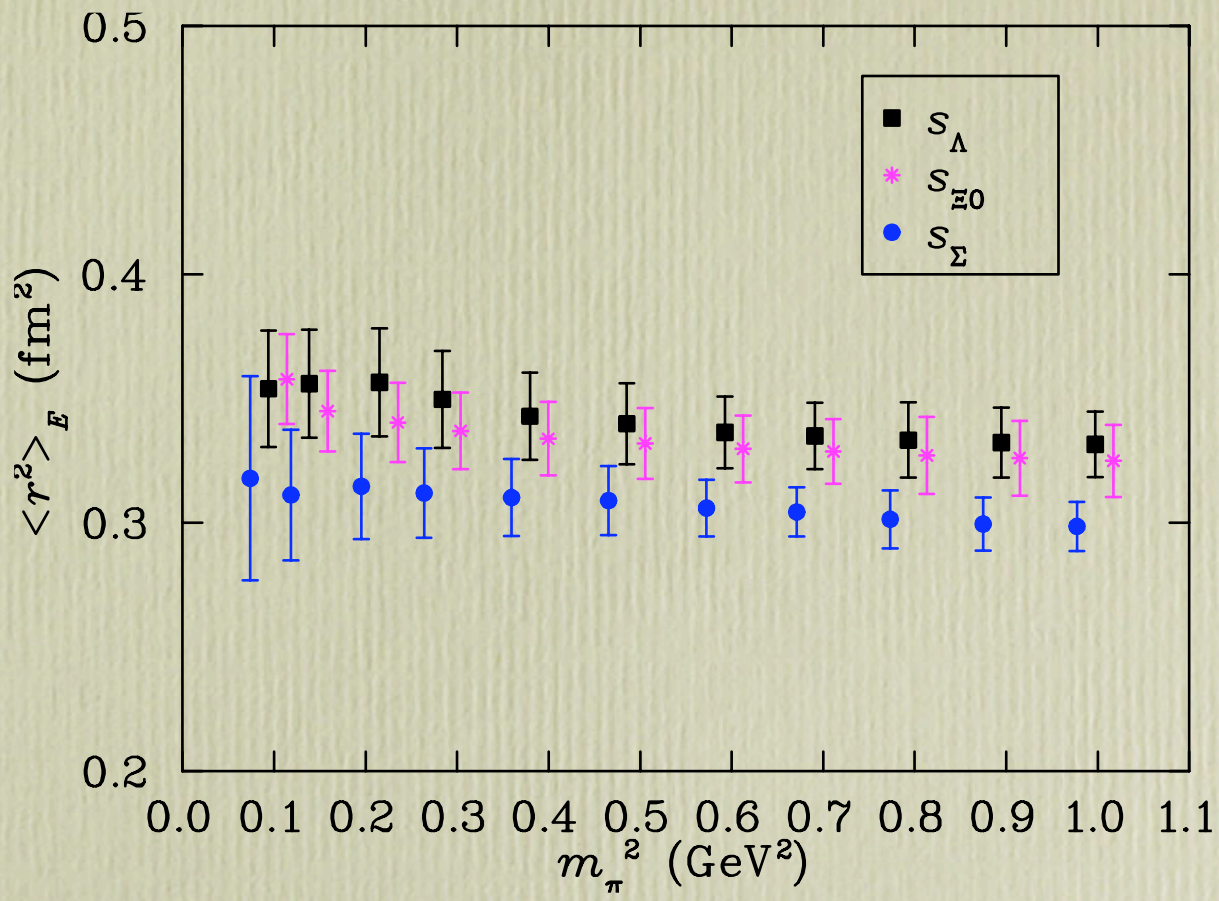

Figure: Electric charge distribution radii of strange quarks including s_Λ, s_{Ξ^0} and s_{Σ^0}. The data for s_{Ξ^0} and s_Λ are plotted at shifted m_π^2 values for clarity. Results are presented for a single quark of unit charge. Note the sensitivity to the environment in which the strange quark sits.

Strange quark magnetic moment

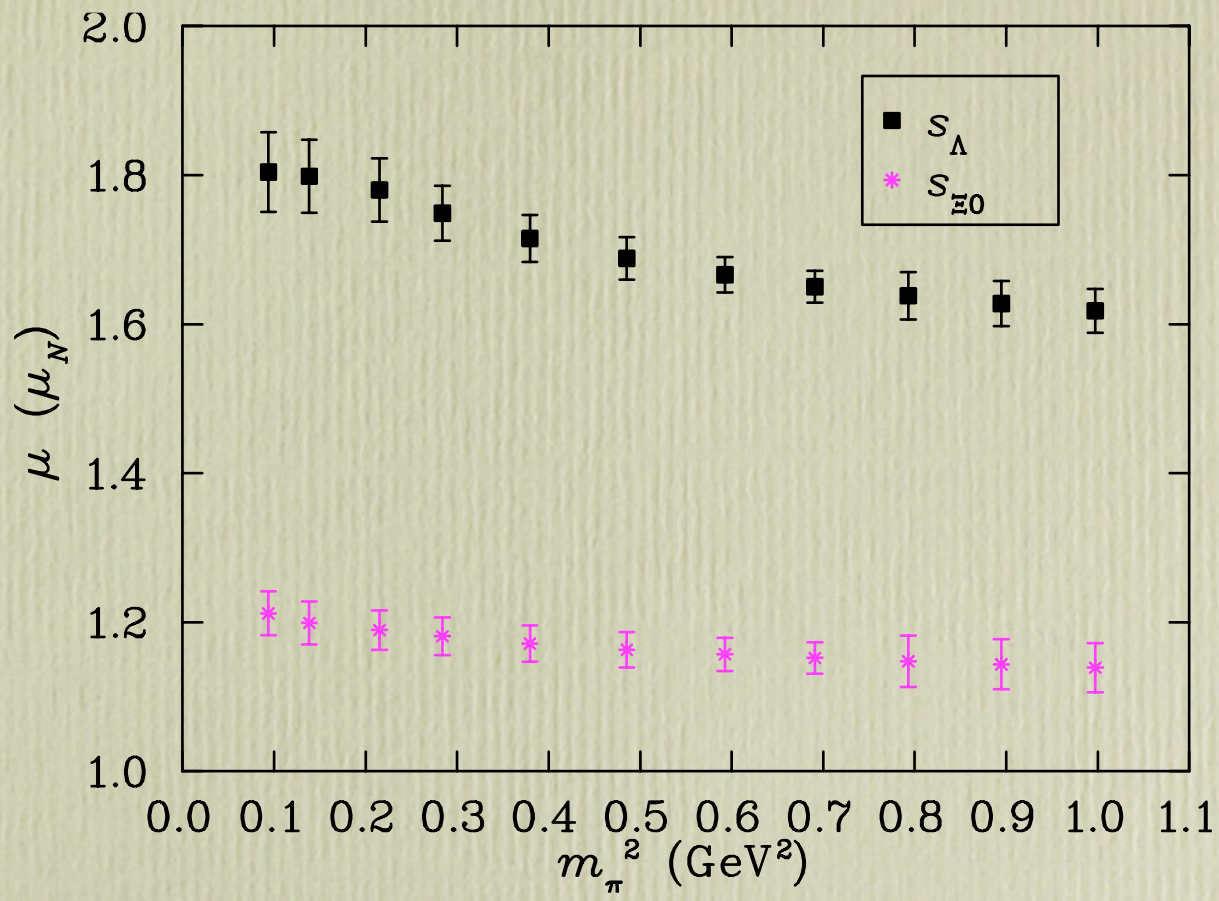

Figure: Magnetic moments of the strange quark in the Λ and the Ξ^0, s_Λ and s_{Ξ^0} respectively, as a function of quark mass. Results are presented for a single quark of unit charge. Note the strong sensitivity of the strange quark to its environment here. The strange quark mass is held fixed, yet the strange quark properties change substantially as the light quark masses change

Magnetic moment of u quark

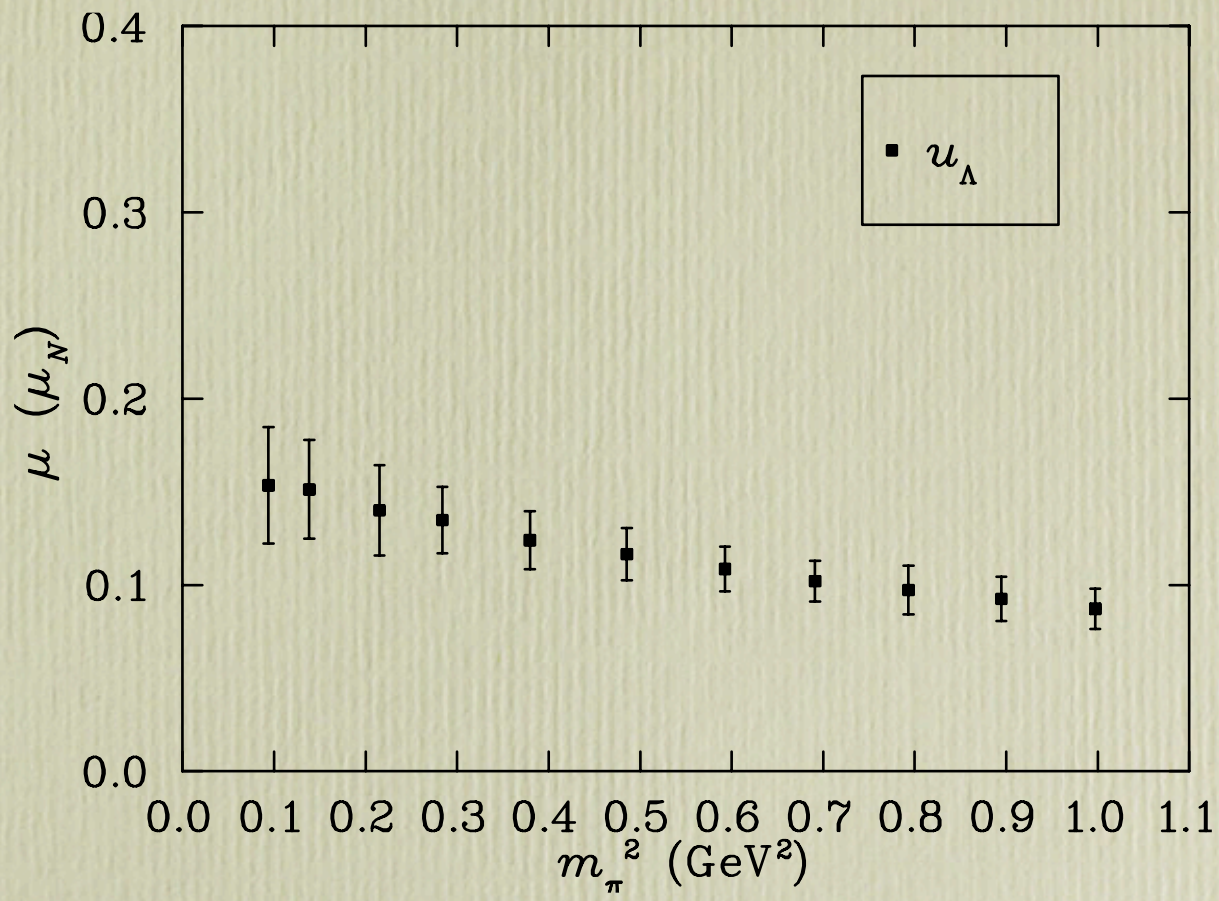

Figure: Magnetic moment contribution of the u-quark sector (or equivalently the d-quark sector) to the Λ^0 magnetic moment. This shows the nontrivial role for light quarks in the Lambda magnetic moment. In simple quark models the light quarks are in a isospin and spin singlet configuration and do not contribute.

Chiral artefact in Delta m.m.

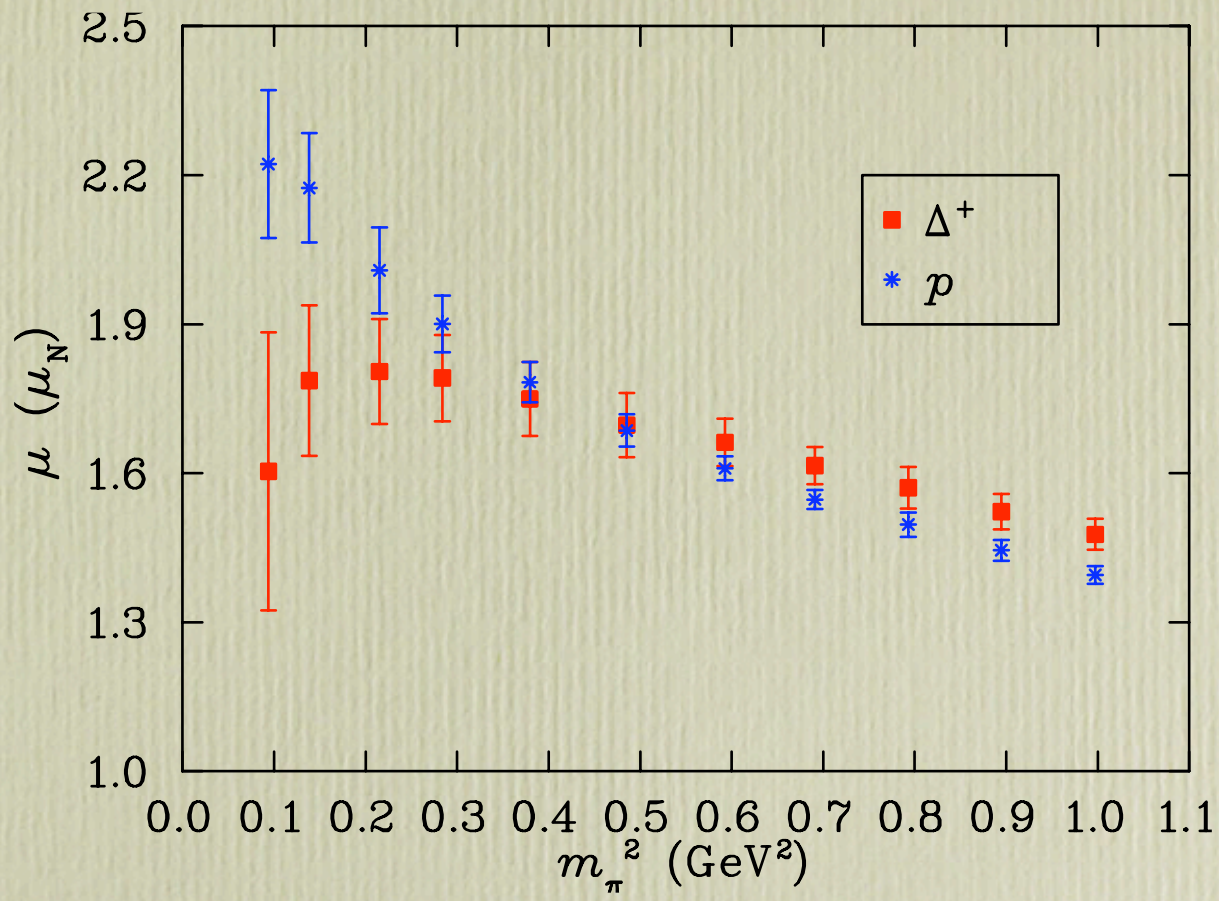

Figure: Comparison of the proton and Δ^+ magnetic moments in quenched QCD with FLIC quarks. Note the evidence of quenched chiral artefacts in the Delta baryon magnetic moment.

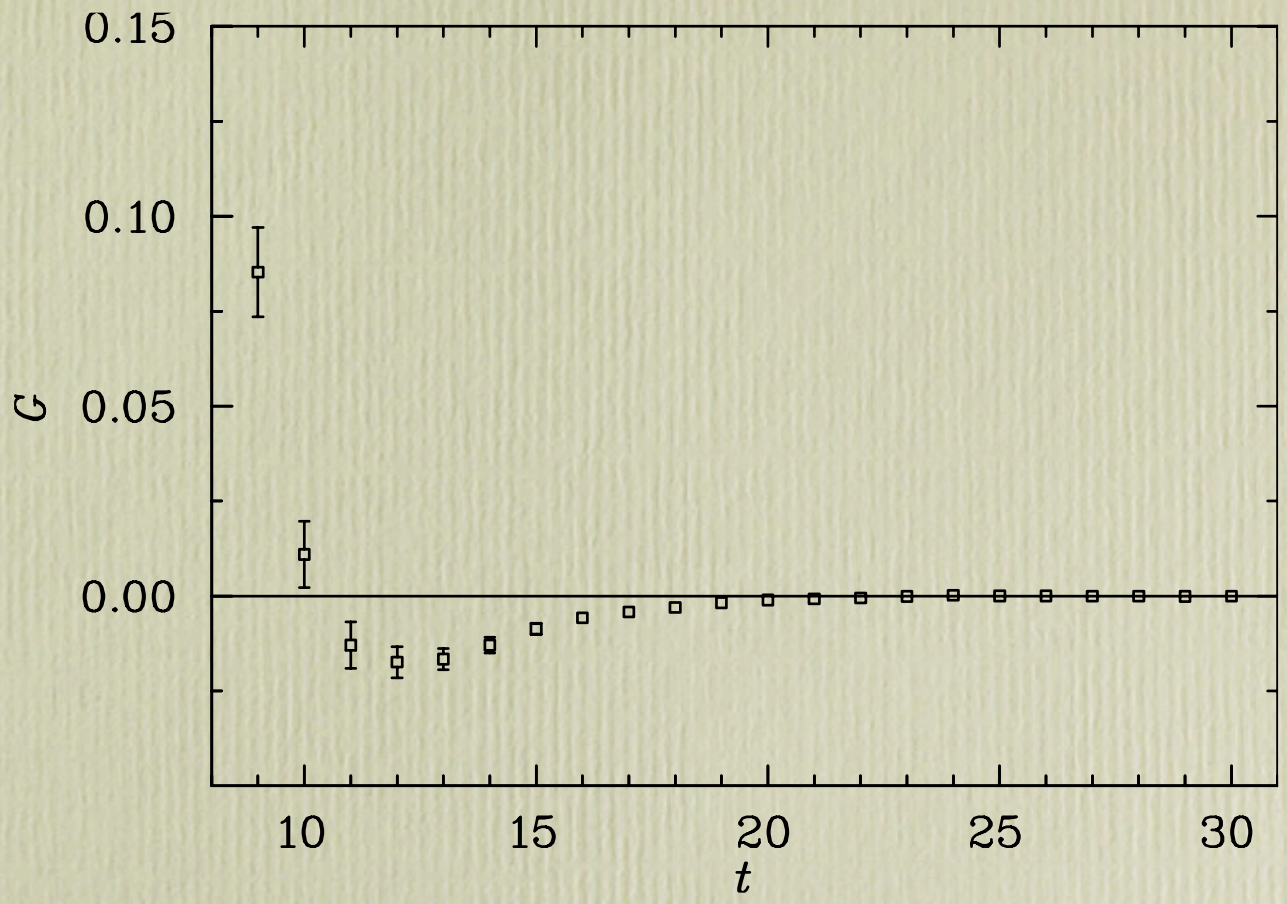

Figure: Evidence of quenching artifacts through the signature of the decay of a_0 to the negative metric π-η' channel is obvious as $G(t)$ changes sign. This is our quenched a_0 meson two-point correlation function for our second lightest quark mass. The signature of the decay of a_0 to the negative metric π-η' channel is obvious as $G(t)$ changes sign.

Hybrid and Exotic Mesons from FLIC Fermions

J.N. Hedditch, B.G. Lasscock, D.B. Leinweber, A.G. Williams, J.M. Zanotti and W. Kamleh

Exotic and Hybrid Mesons

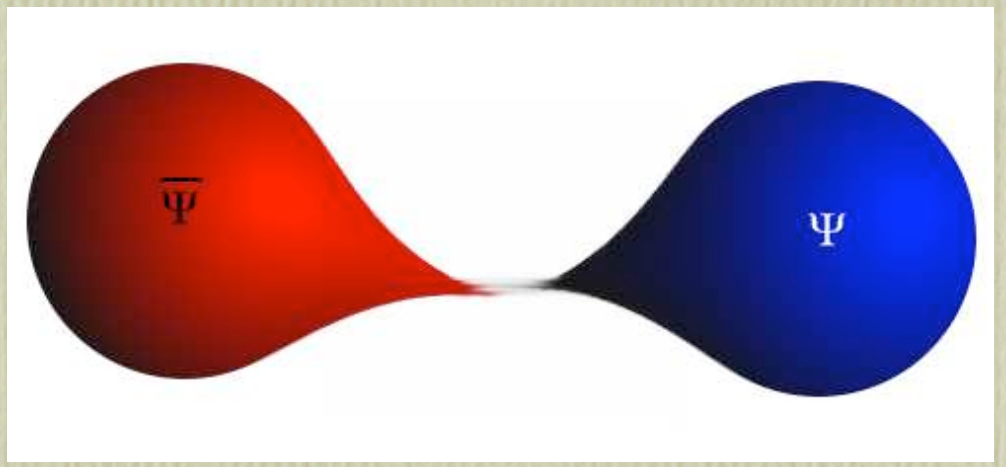

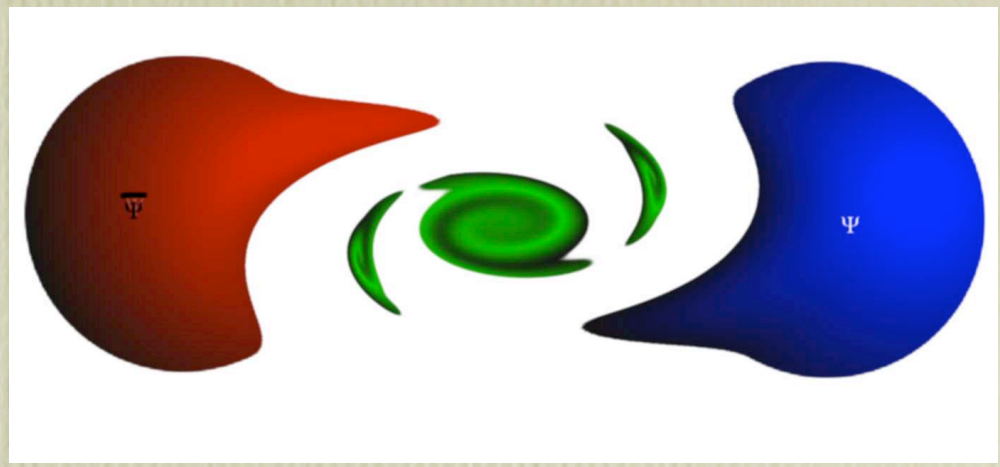

- Exotic mesons are mesons with quantum numbers that cannot be carried by a simple q-$\bar{q}$ pair, e.g., $J^{PC} = 0^{+-}$, 0^{--}, 1^{-+}, etc.
- A hybrid meson is exotic *with* explicit gluon content.
- Major experimental efforts (e.g. GlueX in future Hall D at JLab) aim to search for and probe exotic mesons.
- The 12 GeV upgrade will provide a photon beam to excite flux tubes to produce "explicit glue" in mesons.
- Exotics and hybrids provide a powerful new tool to elucidate aspects of QCD which are relatively unexplored.

Local exotic meson interpolating fields

J^{PC} quantum numbers and their associated meson interpolating fields.

0^{++}	0^{+-}	0^{-+}	0^{--}
$\bar{q}^a q^a$	$\bar{q}^a \gamma_4 q^a$	$\bar{q}^a \gamma_5 q^a$	$-i\bar{q}^a \gamma_5 \gamma_j E_j^{ab} q^b$
$-i\bar{q}^a \gamma_j E_j^{ab} q^b$	$\bar{q}^a \gamma_5 \gamma_j B_j^{ab} q^b$	$\bar{q}^a \gamma_5 \gamma_4 q^a$	
$-\bar{q}^a \gamma_j \gamma_4 \gamma_5 B_j^{ab} q^b$		$-\bar{q}^a \gamma_j B_j^{ab} q^b$	
$-\bar{q}^a \gamma_j \gamma_4 E_j^{ab} q^b$		$-\bar{q}^a \gamma_4 \gamma_j B_j^{ab} q^b$	

1^{++}	1^{+-}	1^{-+}	1^{--}
$-i\bar{q}^a \gamma_5 \gamma_j q^a$	$-i\bar{q}^a \gamma_5 \gamma_4 \gamma_j q^a$	$\bar{q}^a \gamma_4 E_j^{ab} q^b$	$-i\bar{q}^a \gamma_j q^a$
$i\bar{q}^a \gamma_4 B_j^{ab} q^b$	$i\bar{q}^a B_j^{ab} q^b$	$-\epsilon_{jkl} \bar{q}^a \gamma_k B_l^{ab} q^b$	$\bar{q}^a E_j^{ab} q^b$
$i\epsilon_{jkl} \bar{q}^a \gamma_k E_l^{ab} q^b$	$\bar{q}^a \gamma_5 E_j^{ab} q^b$	$\epsilon_{jkl} \bar{q}^a \gamma_4 \gamma_k B_l^{ab} q^b$	$-i\bar{q}^a \gamma_5 B_j^{ab} q^b$
$i\epsilon_{jkl} \bar{q}^a \gamma_k \gamma_4 E_l^{ab} q^b$	$\bar{q}^a \gamma_5 \gamma_4 E_j^{ab} q^b$	$-i\epsilon_{jkl} \bar{q}^a \gamma_5 \gamma_4 \gamma_k E_l^{ab} q^b$	$i\bar{q}^a \gamma_4 \gamma_5 B_j^{ab} q^b$

- We consider the local interpolating fields summarized in previous table
- Gauge-invariant Gaussian smearing applied at the fermion source (t = 8), and local sinks are used to maintain strong signal in the two-point correlation functions.
- Chromo-electric and -magnetic fields created from 3-D APE-smeared links at source and sink using the highly-improved $O(a^4)$ -improved field strength tensor

A fixed boundary condition in the time direction is used for the fermions by setting $U_t(\vec{x}, N_t) = 0 \; \forall \; \vec{x}$ in the hopping terms of the fermion action, with periodic boundary conditions imposed in the spatial directions.

Eight quark masses are considered in the calculations and the strange quark mass is taken to be the third heaviest quark mass. This provides a pseudoscalar mass of 697 MeV which compares well with the experimental value of $(2M_K^2 - M_\pi^2)^{1/2} = 693\,\mathrm{MeV}$ motivated by leading order chiral perturbation theory.

Results survey for 1^{-+} meson

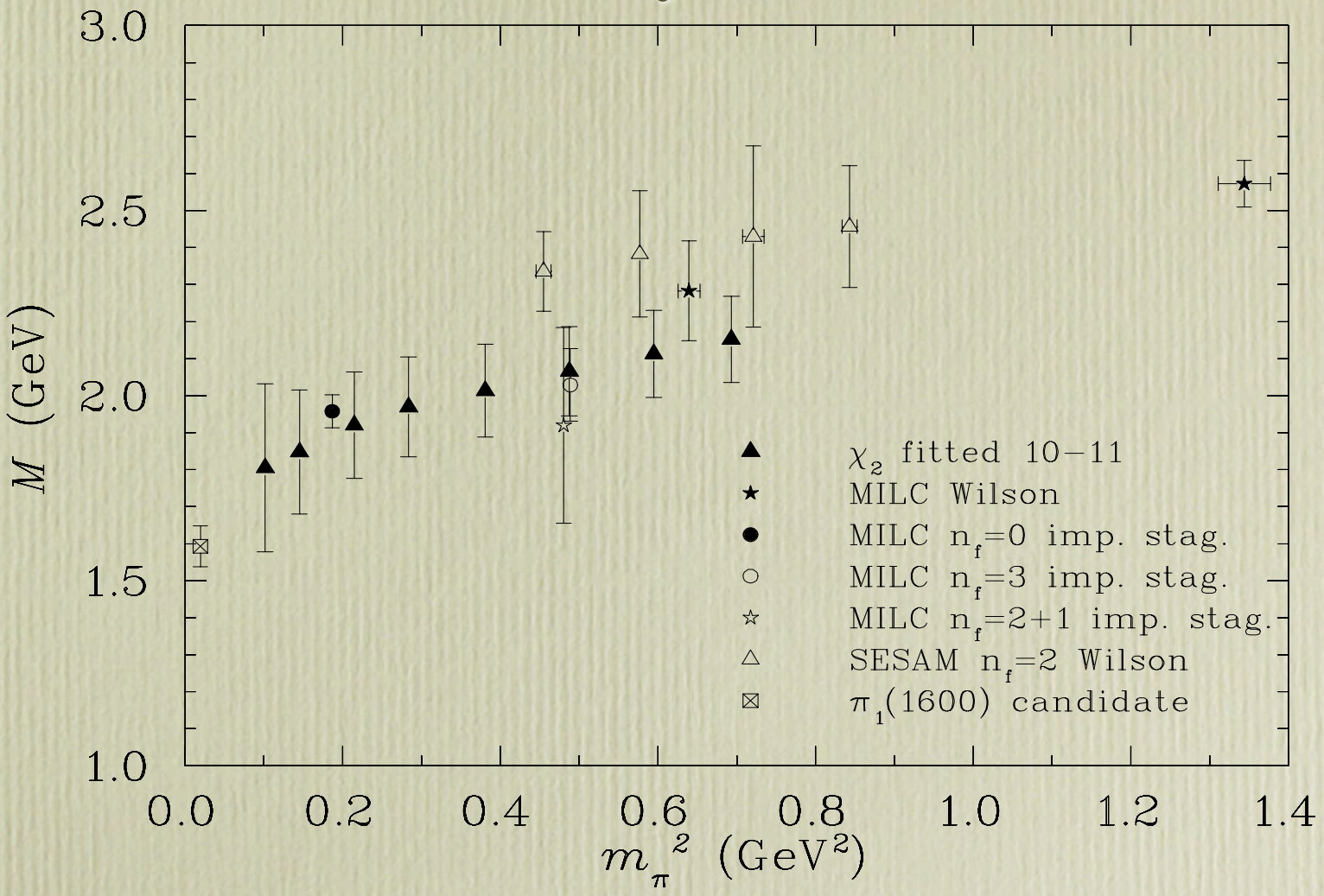

Fig. 3.5: A survey of results in this field. The MILC results are taken from [7] and show their $Q^4, 1^{-+} \rightarrow 1^{-+}$ results, fitted from $t = 3$ to $t = 11$. Open and closed symbols denote dynamical and quenched simulations respectively.

1^{-+} meson vs its decay channel

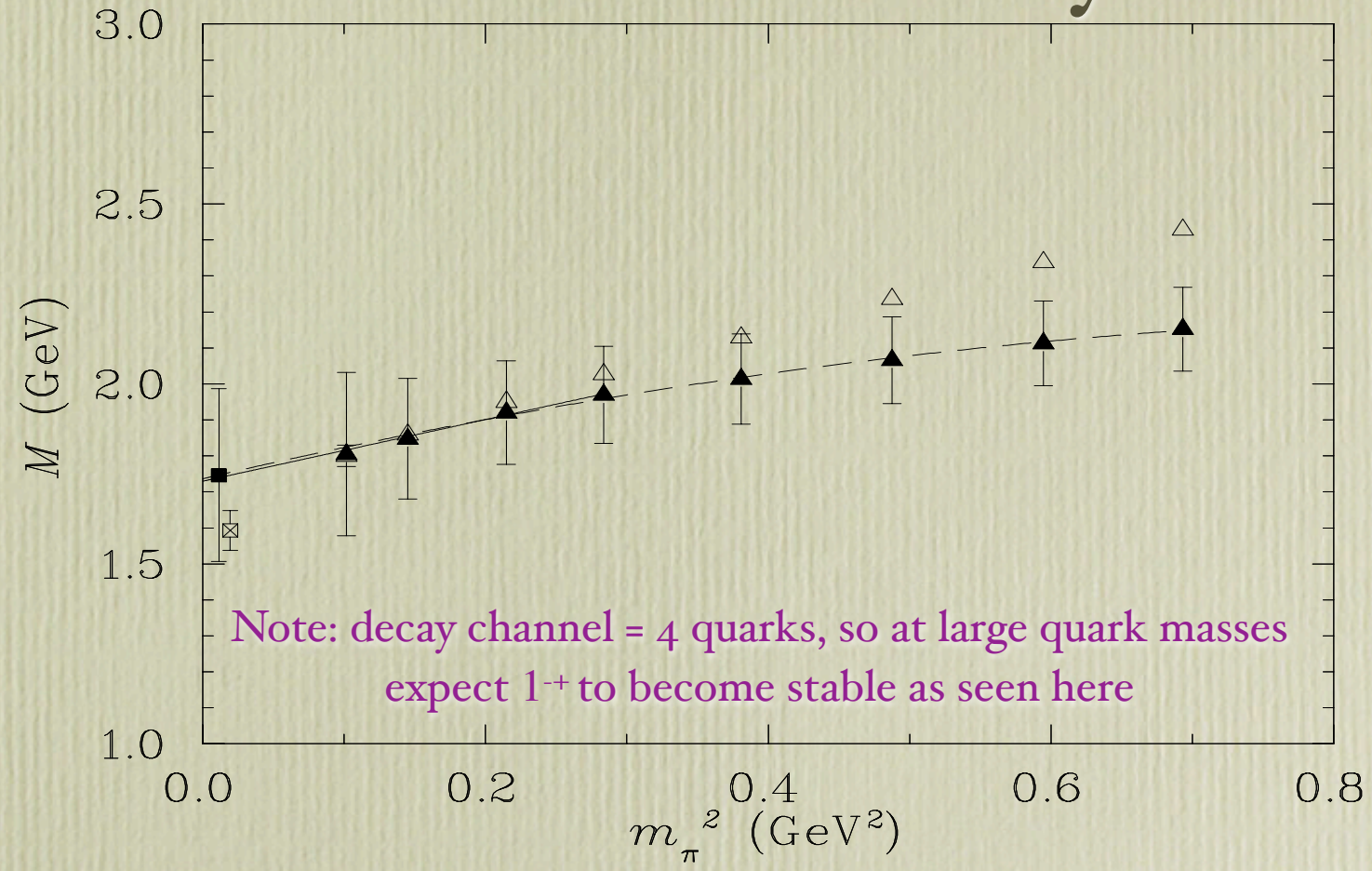

Fig. 3.6: The 1^{-+} exotic meson mass obtained from fits of the effective mass of the hybrid interpolator χ_2 from $t = 10 \rightarrow 12$ (full triangles) are compared with the $a_1\eta'$ two-particle state (open triangles). The extrapolation curves include a quadratic fit to all eight quark masses (dashed line) and a linear fit through the four lightest quark masses (solid line). The full square is result of linear extrapolation to the physical pion mass, while the open square (offset for clarity) indicates the $\pi_1(1600)$ experimental candidate. .

Quark and Gluon Propagators in Full QCD

M.B. Parappilly, P.O. Bowman, U.M. Heller, D.B. Leinweber, A.G. Williams, J.B. Zhang

Abstract. We present an unquenched calculation of the quark propagator in Landau gauge with 2+1 flavors of dynamical quarks. We study the scaling behavior of the quark propagator in full QCD on two lattices with different lattice spacings and similar physical volume. We use configurations generated with an improved staggered ("Asqtad") action by the MILC collaboration.

Details of simulations

TABLE 1. Lattice parameters used in this study. The dynamical configurations each have two degenerate light quarks (up/down) and a heavier quark (strange).

Dimensions	β	a	**Bare Quark Mass**	**#Config**
$28^3 \times 96$	7.09	0.090 fm	14.0 MeV, 67.8 MeV	108
$28^3 \times 96$	7.11	0.090 fm	27.1 MeV, 67.8 MeV	110
$20^3 \times 64$	6.76	0.125 fm	15.7 MeV, 78.9 MeV	203
$20^3 \times 64$	6.79	0.125 fm	31.5 MeV, 78.9 MeV	249
$20^3 \times 64$	6.81	0.125 fm	47.3 MeV, 78.9 MeV	268
$20^3 \times 64$	6.83	0.125 fm	63.1 MeV, 78.9 MeV	318

Quenched vs Unquenched

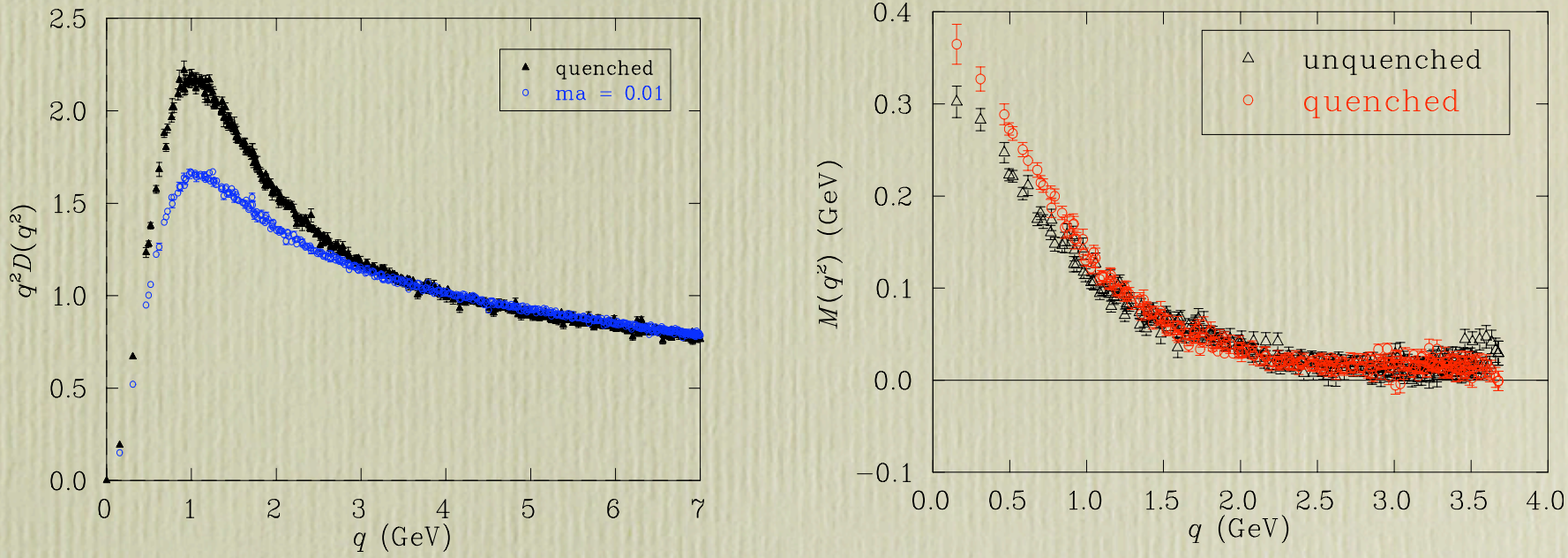

FIGURE 1. The gluon dressing function in Landau gauge is left. Full triangles correspond to the quenched calculation, while open circles correspond to 2+1 flavor QCD. As the lattice spacing and volume are the same, the difference between the two results is entirely due to the presence of quark loops. Right is the comparison of the unquenched (full QCD) and quenched quark propagator for non-zero quark mass. The mass function for the unquenched dynamical-fermion propagator has been interpolated so that it agrees with the quenched mass function for $ma = 0.01$ at the renormalization point, $q = 3$ GeV. For the unquenched propagator this corresponds to a bare quark mass of $ma = 0.0087$.

Note that the effect of unquenching is to move propagators toward their tree-level form, i.e., more Abelian-like as expected naively

Scaling of quark propagator

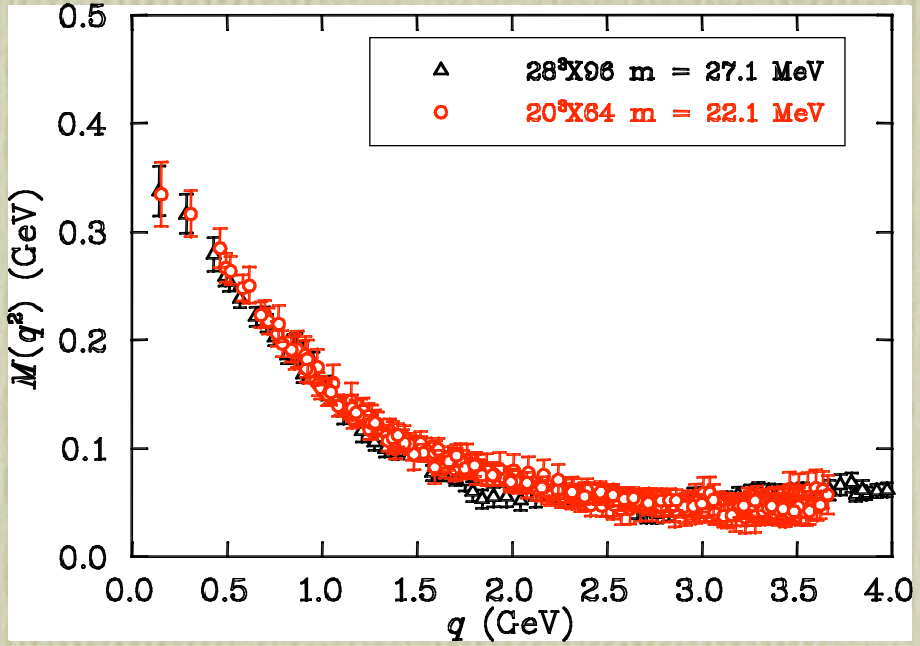

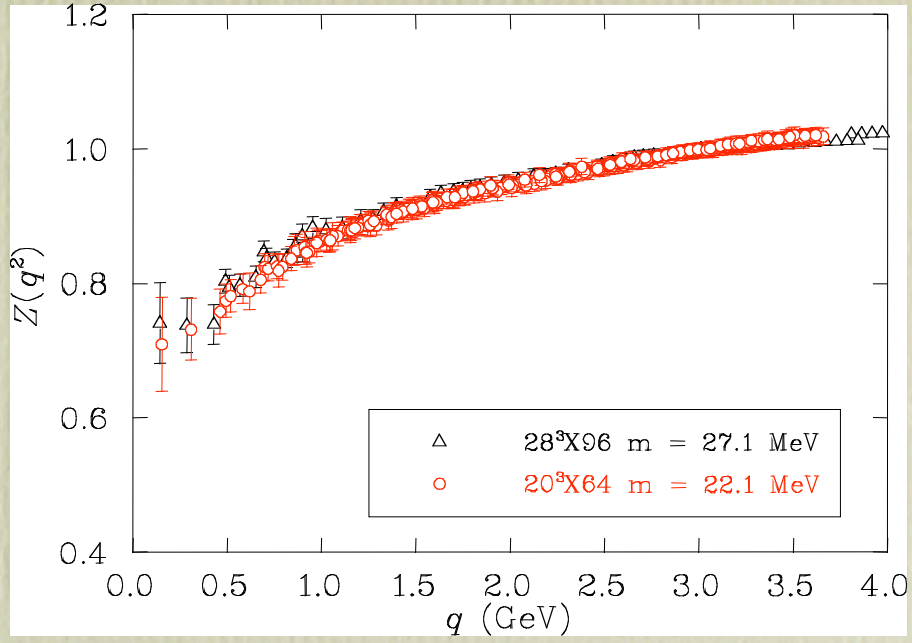

Test of scaling for full QCD (i.e., unquenched) quark propagator:

- Quark propagator is a fundamental quantity in QCD. Shows nonperturbative behavior such as mass generation explicitly.
- Comparison of wave-function renormalization function $Z(q^2)$ and mass function $M(q^2)$ for two different 2+1 flavor MILC lattices renormalized to agree at 3 GeV and with similar volumes.
- The triangles corresponds to a $28^3 \times 96$ lattice with spacing $a = 0.09$ fm, while the open circles are for a $20^3 \times 64$ lattice with spacing $a = 0.125$ fm (obtained by interpolating four different set of light quark masses).

Good scaling is seen!

Conclusions

- The CSSM continues to do well in its post "block funding" era. (Note: future Cairns workshops may be a little more difficult ...)
- Range of results shown by Ben, Derek and I are a good sample of current lattice research efforts: baryon masses and pentaquarks, flux tubes and QCD vacuum, e.m. structure of octet, exotics and hybrids, unquenched quark and gluon propagators, ...
- Future may include finite T and density, unquenched simulations, and other activities.
- New computer to arrive by end of year will help.